

Using Spectroscopic Data on Imidazolium Cation Conformations To Test a Molecular Force Field for Ionic Liquids

José N. A. Canongia Lopes*

Centro de Química Estrutural, Instituto Superior Técnico, 1049-001 Lisboa, Portugal and Instituto de Tecnologia Química e Biológica, Oeiras, Portugal

Agílio A. H. Pádua

Laboratoire de Thermodynamique des Solutions et des Polymères, Université Blaise Pascal Clermont-Ferrand/CNRS, 63177 Aubière, France

Received: December 27, 2005; In Final Form: February 10, 2006

A molecular force field for the computer simulation of ionic liquids is evaluated a posteriori by confrontation against Raman spectroscopic data, published after the force field had been formulated. Specifically, the terms in the force field describing the conformational aspects of dialkylimidazolium cations, which were specifically developed for these compounds using high level ab initio calculations, are those affecting the distribution of conformers in simulated ionic liquids. Those distributions are compared with analyses of the liquid-phase Raman spectra, and the features of a series of dihedral torsions along the alkyl side chains in 1-alkyl-3-methylimidazolium cations in several ionic liquids are discussed.

Introduction

The development in the past few years of different molecular models for ionic liquids^{1–5} (ILs) to be used within the framework of statistical mechanics simulations was received with great interest by many researchers who can use those models to study structural, energetic, and dynamic properties of ionic liquids. So far, ILs composed of alkylimidazolium cations have been the most widely studied. The molecular force fields are presented in the familiar OPLS-AA or AMBER form with some parameters taken directly from the existing literature, thus transferred from other molecules, and other parameters developed specifically for the ILs. These force fields are understood within the molecular mechanics approximation, describing the potential energy as a sum of bonded (intramolecular) and nonbonded (intra- and intermolecular) terms. Bonded contributions arise from covalent bonds, valence angles, and dihedral torsions; nonbonded contributions are of the Lennard–Jones type plus partial charges or other similar forms. The distribution of electrostatic charges among the interaction sites in the ions is the class of parameter that has been adjusted by all of the authors proposing a force field.^{3–5} However, only two of the models in the literature^{1,2} were parametrized specifically against ab initio calculations of the torsion energy profiles in imidazolium cations, therefore yielding an accurate description of the conformational characteristics of these ions.

The evaluation of molecular force fields against experimental data remains a critical issue, and any new experimental data that can be used to assist on that assessment is always of crucial importance. In a recent publication, Umebayashi and co-workers⁶ confirmed using Raman spectroscopy and quantum chemical calculations that the 1-ethyl-3-methylimidazolium cation (C_2mim^+ , Figure 1), present in several ionic liquids, exists as a mixture of two principal conformers shown in Figure 2 a,b. The two conformers are obtained by rotation around the $C2-N1-C6-C7$ dihedral angle. The results of these authors

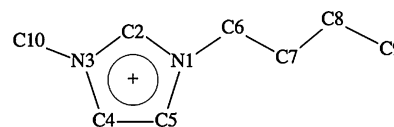


Figure 1. Nomenclature of 1-alkyl-3-methylimidazolium cations. The example shown is C_4mim^+ .

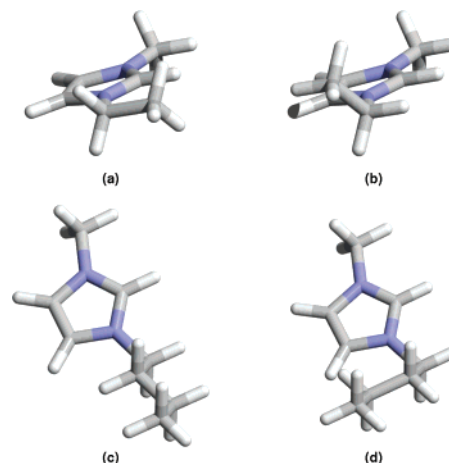


Figure 2. Identification of the different conformers in the 1-ethyl-3-methylimidazolium cation and in the 1-butyl-3-methylimidazolium cation: (a) C_2mim^+ planar, (b) C_2mim^+ nonplanar, (c) C_4mim^+ C1–C2 anti, (d) C_4mim^+ C1–C2 gauche.

also support the soundness of the approximations used when we developed a systematic molecular force field for ILs,¹ namely the detailed mapping of the torsion profile around the above-mentioned dihedral angle.

In other recent publications, Osawa et al.,⁷ Katayanagi et al.,⁸ and Berg et al.⁹ also demonstrated the existence of conformers for the 1-butyl-3-methylimidazolium cation (C_4mim^+) in ionic liquids containing tetrafluoroborate,⁷ halide,^{8,9} and hexafluorophosphate⁹ anions, shown in Figure 2c,d. The conformations

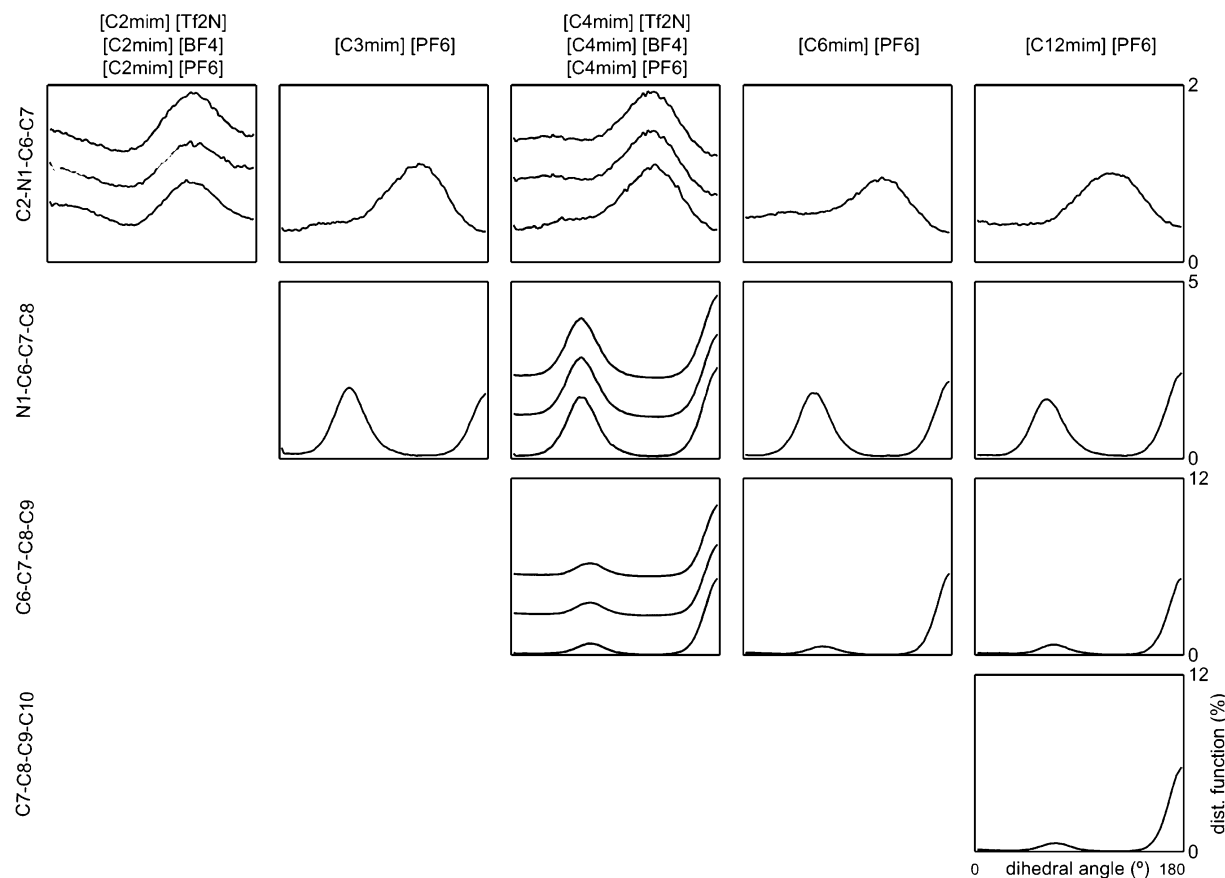


Figure 3. Dihedral distribution functions obtained by MD simulation at 300 K. The graphs with multiple ionic liquids (different anions) are shifted in relation to the bottom ionic liquid/line to make the graph more readable.

studied in C_4mim^+ were those around the C6–C7 bond, i.e., the N1–C6–C7–C8 dihedral. Berg et al.⁹ also extended their investigation to the 1-hexyl-3-methylimidazolium cation (C_6mim^+) in ILs with chloride and hexafluorophosphate anions and observed similar conformers around the C6–C7 bond.

In this work, we will proceed to test *a posteriori* the molecular force field previously published¹ using the spectroscopic data of Umebayashi et al.⁶ and of Berg et al.⁹ The condensed phase dihedral distributions, and their temperature dependence, obtained from these authors' experimental data will be confronted with the results of molecular dynamics (MD) calculations using our force field.

Simulation Methods

All of the ILs studied were modeled by the all-atom molecular force field proposed by us in two previous publications.^{1,10} This force field is based on the OPLS-AA/AMBER framework, but it was to a large extent developed specifically for ionic liquids. While developing the force field it was always our reasoning that accurate conformational energies and electrostatic charge distributions derived from high-level quantum calculations would be relevant to render subtle energetic or configurational features, such as those responsible for many of the particular properties of these large organic salts in the liquid phase.

The molecular dynamics (MD) runs were performed using the DL_POLY program¹¹ on cubic boxes at $T = 300$ K with the usual boundary conditions. Different system sizes were considered, containing 256, 500, and 700 ions; for example, in $[C_6mim][PF_6]$ the large system corresponds to simulations with 13600 atoms. Ewald summation and the usually employed long-range corrections for the dispersion forces accounted for the

interaction beyond the explicit cutoff of 16 Å. Equilibrations starting from a low-density random arrangement of ions were performed during 500 ps. They were followed by trajectories of 500 ps at constant (N, p, T). The simulation times and system sizes chosen were verified for the convergence and significance of equilibrium properties such as densities, energies, and radial distribution functions.

Results and Discussion

The MD simulation results generated configuration data from which dihedral angle distributions could be calculated. To obtain these histograms, 1000 configurations were considered from the equilibrated trajectory (each configuration 5 ps apart from the previous one) for each ionic liquid, and then dihedral angle distribution histograms were built with a resolution of two degrees. The results are gathered in Figure 3.

For C_2mim^+ , the histograms show (Figure 3, upper left corner) that there are two preferred conformers: the first corresponds to a C2–N1–C6–C7 dihedral angle of 0° giving a planar conformation, Figure 2a, while the second corresponds to a nonplanar conformation with a dihedral angle of approximately 120°, Figure 2b. These results agree with both the *ab initio* calculations of Umebayashi et al.—that predict minima in the torsion energy profile around 0 and 110° (see Figure 3 of ref 6)—and also with their Raman experimental data that give evidence for the two conformers in the liquid phase: the spectra exhibit peaks at 387 and 430 cm^{-1} characteristic of the nonplanar conformation and also at 448 cm^{-1} characteristic of the planar conformer (see Figure 2 of ref 6). A more quantitative analysis of the three sets of data (MD, *ab initio*, and Raman) was performed with the results shown in Table 1.

TABLE 1: Relative Amounts of the Planar (P) and Nonplanar (NP) Conformers of the 1-Ethyl-3-methylimidazolium Cation in Different Ionic Liquids, Estimated Using Experimental Spectroscopic Raman Data, Molecular Dynamics (MD) Simulations, and ab Initio (AI) Calculations^a

	a_1/a_2	h_1/h_2	NP/P(<i>a</i>)	$x_P(a)$	NP/P(<i>h</i>)	$x_P(h)$
Raman data ^b						
[C ₂ mim][BF ₄]	3.12	1.26	8.60	0.10	3.48	0.22
MD data						
[C ₂ mim][PF ₆]			2.38	0.30	2.67	0.27
[C ₂ mim][Tf]			2.25	0.31	2.67	0.27
[C ₂ mim][Tf ₂ N] (L)			4.07	0.20	3.39	0.23
[C ₂ mim][Tf ₂ N] (S)			2.36	0.30	3.00	0.25
AI data ^c						
C ₂ mim ⁺		0.36			5.06	0.17

^a The anions Tf⁻ and Tf₂N⁻ stand for trifluoromethyl sulfate CF₃SO₃⁻ and bis(trifluoromethanesulfonyl)amide (CF₃SO₂)₂N⁻, respectively. Headings a_i/a_j refer to peak area ratios; h_i/h_j to peak intensity ratios; and x_P (*a* or *h*) refer to the fraction of the planar conformer calculated using either area or intensity ratios. Double MD entries refer to larger (L) and smaller (S) systems. ^b Peak 1 is the average of peaks at 387 and 430 cm⁻¹ (NP); peak 2 at 448 cm⁻¹ (P), ref 6. ^c Peak 1 is the average of peaks at 380 and 419 cm⁻¹ (NP); peak 2 at 444 cm⁻¹ (P), ref 6.

Based on the Gaussian decomposition of the Raman spectrum of [C₂mim][BF₄] (presented in Figure 4 of ref 6), we estimated the ratio between the areas (a_1/a_2) and the heights (h_1/h_2) of the peaks characteristic of the planar and nonplanar conformers. These values were then corrected by the ratio of the Raman intensities estimated ab initio to yield the ratio between the populations of the two conformers, NP/P(*a*) and NP/P(*h*), respectively, and the corresponding fractions of the planar conformer, $x_P(a)$ and $x_P(h)$. These results, which are 0.10 and 0.22, respectively, are not entirely consistent, reflecting the crude approximations implied in the attempt to estimate relative amounts of the conformers from Raman spectra. The Raman intensities estimated ab initio refer to calculations performed on an isolated molecule at a given conformation, and not to the distribution of conformers that exist in the condensed phase. Moreover, the widening of the bands in the condensed phase is not taken into account. However, even if approximate, the calculations from the spectra provide a rough estimate that can be compared (semiquantitatively) with the values obtained from the other two sets of data.

From the MD data, the ratio between the two conformers and the fraction of the planar one can be calculated from a Gaussian decomposition of the histograms presented in Figure 3. For all of the ILs simulated by MD, the fractions of the planar conformer range from 0.20 to 0.30 and are given in Table 1.

The Gibbs free energy difference between the two isomers, ΔG , obtained ab initio (Table 1 from ref 6) can also serve to derive the relative amounts of the two conformers. A $\Delta G = 2.3$ kJ mol⁻¹ (the nonplanar conformer is more stable) corresponds to a fraction of the planar conformer of 0.17. It must be stressed at this point that, since there are two possible enantiomeric nonplanar conformations but only one planar conformation, a factor of 2 must be used when calculating the relative amounts of the two conformers.

The three sets of data yield similar results, showing that there is a larger amount of nonplanar conformer (around 80%). This is a remarkable (albeit semiquantitative) agreement since the confrontation of data from single-molecule calculations (ab initio) with condensed-phase results (MD and Raman) can sometimes lead to erroneous results. The same conclusion applies to the comparison between MD results, based on a

semiempirical force field, and the attempt to extract quantitative data from the intensity and width of peaks of a Raman spectra.

Finally, Umebayashi et al.⁶ also concluded that, as the temperature was raised, the amount of the planar conformer would increase, which is in agreement with the ab initio predictions of the value of the enthalpy difference, ΔH , between the two conformers. Although no quantitative estimation of this property was made from the MD data, the histograms show that as the temperature is increased the distribution of dihedral angles is modified, with an increase of the relative amount of the planar conformer.

Two remaining issues concerning the C2–N1–C6–C7 must be addressed (cf. first row of histograms in Figure 3). First, when one moves from C₂mim⁺ to longer alkyl side chains, the peak at 0° (planar conformation) disappears. This means that from the energetic point of view, the local minimum in the torsion energy profile of this dihedral angle is overcome by the contribution of nonbonded interactions arising from atoms in the longer alkyl chain. This situation is already present in C₃mim⁺ and remains unaltered with the longer alkylmethylimidazolium cations, as seen in the histograms for C₄mim⁺, C₆mim⁺, and C₁₂mim⁺. Second, all C2–N1–C6–C7 histograms show nonnegligible populations at all conformations, and not just for the values of the dihedral around the two energy minima. In the simulated liquid phase there is a wide distribution of conformers, with two peaks at the planar and nonplanar conformations, implying a considerable freedom of rotation around the N1–C6 bond. This situation is also present when the cation contains a longer alkyl chain.

For the C₃mim⁺, C₄mim⁺, C₆mim⁺, and C₁₂mim⁺ cations, a similar analysis can be conducted, but now centered on the distribution of the N1–C6–C7–C8 dihedral. The histograms for this dihedral angle are shown in the 2nd row of Figure 3, and they exhibit two peaks: one at 180° corresponding to an anti (*a*-) conformer, Figure 2c, and one around 60° corresponding to a gauche (*g*-) conformer, Figure 2d. These results agree with both our own ab initio calculations performed when developing the force field—that predict minima in the torsion energy profile around the same angles (Figure 3 of ref 1)—and also with the experimental Raman data of Berg et al.⁹ that show evidence for the two conformers in the liquid phase: for instance, the liquid-phase spectra exhibit peaks around 625 cm⁻¹ characteristic of the anti conformation and around 600 cm⁻¹ characteristic of the gauche conformers (Tables 2 and 6 of ref 9). Again, a more quantitative analysis of the three sets of data (MD, AI, Raman) was performed, the results of which are given in Table 2.

The ab initio calculations performed by Berg et al.⁹ predicted a relatively small difference between the Gibbs free energy of the two conformers: ΔG around only 0.2 kJ mol⁻¹, the anti and gauche conformers being the more stable in the case of C₄mim⁺ and C₆mim⁺, respectively. With such a low free energy difference, the ratio of anti/gauche should be approximately 2:1, since there are two gauche and one anti conformers, corresponding to a fraction of anti conformer of about 0.33 (cf. last two rows of Table 2). For this dihedral angle, the peak ratio measurements at the characteristic frequencies of the anti and gauche conformers, again by Gaussian decomposition of the appropriate portion of the Raman spectra, yield results that are inconsistent with this last result, giving a fraction of the anti conformer around 0.65. Nevertheless, the Raman data clearly show the existence of both conformers in the ionic liquid. The inconsistency between the Raman spectra and the ab initio calculations of free energy can probably be assigned to the rather

TABLE 2: Relative Amounts of the Anti (A) and Gauche (G) Conformers of the 1-Butyl-3-methylimidazolium and 1-Hexyl-3-methylimidazolium Cations Contained in Different Ionic Liquids, Estimated Using Experimental Spectroscopic Raman Data, Molecular Dynamics (MD) Simulations, and ab Initio (AI) Calculations^a

	a_1/a_2	H_1/H_2	A/G (a)	x_A (a)	A/G (h)	x_A (h)
Raman data ^b						
[C ₄ mim][PF ₆]	1.94	1.30	0.84	0.54	0.56	0.64
[C ₄ mim][BF ₄]	1.71	1.23	0.74	0.58	0.53	0.65
[C ₆ mim][Cl]	1.31	1.10	0.63	0.61	0.53	0.65
[C ₆ mim][PF ₆]	1.53	1.16	0.74	0.58	0.56	0.64
MD data						
[C ₄ mim][PF ₆] (S)			1.26	0.44	1.38	0.42
[C ₄ mim][PF ₆] (L)			1.61	0.38	1.78	0.36
[C ₄ mim][BF ₄] (S)			1.32	0.43	1.48	0.40
[C ₄ mim][BF ₄] (L)			1.55	0.39	1.67	0.38
[C ₄ mim][Tf ₂ N] (S)			1.34	0.43	1.48	0.40
[C ₄ mim][Tf ₂ N] (L)			1.50	0.40	1.58	0.39
[C ₆ mim][PF ₆]			1.60	0.38	1.69	0.37
AI data ^c						
C ₄ mim ⁺	2.07				2.15	0.35
C ₆ mim ⁺	2.31				1.87	0.32

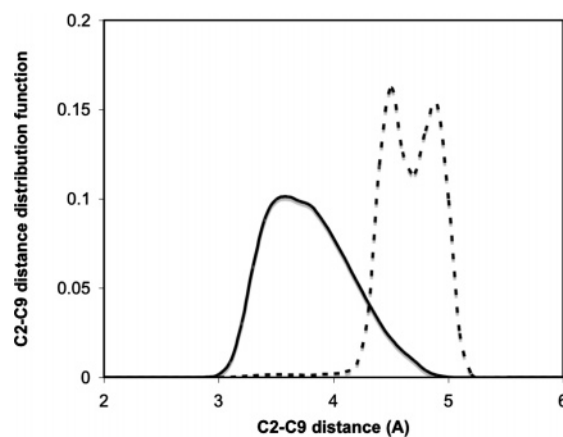
^a The nomenclature is similar to that used in Table 1. Double MD entries refer to larger (L) and smaller (S) systems. ^b Peak 1 at 601 cm⁻¹ (G); peak 2 at 625 cm⁻¹ (A), ref 9. ^c Peak 1 at 604 cm⁻¹ (G); peak 2 at 637 cm⁻¹ (A), ref 9.

rudimentary approximations involved in the estimation of the relative amounts of each conformer from the Raman peaks, and also to the use in the ab initio calculations of just two conformations of one isolated molecule, and not of the continuous distribution that in fact exists in condensed phase, including the rather diffuse distribution of the C2–N1–C6–C7 dihedral angle.

The MD calculations yield two distinctive peaks, seen in the second row of Figure 3. The ratios (area and intensity) of these two peaks correspond to fractions of the anti conformer around 0.40 for C₄mim⁺ and 0.37 for C₆mim⁺, values that are comparable to the ones estimated ab initio. The N1–C6–C7–C8 dihedral angle distributions calculated by the MD simulations also show that, unlike for the C2–N1–C6–C7 distribution, the molecules in the liquid phase are clearly either in the anti or in the gauche conformation around the C6–C7 bond, with negligible amounts of intermediate conformations. This trend is already present in C₃mim⁺ and extends up to C₁₂mim⁺, as can be observed in the second row of Figure 3.

A final remark can be made about the dihedrals further away from the imidazolium ring along the alkyl side chain, whose histograms are presented in the last rows of Figure 3. The dihedral angle distributions in these cases exhibit pronounced peaks corresponding to anti conformers and much less intense ones associated with gauche conformers, as is typical of normal alkanes.¹² This behavior is present for all C–C–C–C torsions, from the first of such dihedral angles in C₄mim⁺ to the one at the end of the side chain in C₁₂mim⁺ (lower right corner of Figure 3). The significant differences between the C–C–C–C and the N1–C6–C7–C8 dihedrals lead us to conclude that the latter must be parametrized in a specific manner for imidazolium cations and cannot be reliably extrapolated from other families of molecule.

It must be stressed at this point that Margulis et al.¹³ also calculated dihedral distributions on similar ionic liquid systems using MD simulation data. However, the employed force field was not specifically developed to account for the torsional energy profiles of alkyl chains linked to imidazolium rings (OPLS parameters for normal alkyl chains were used) which means that we did not use it for comparison purposes.

**Figure 4.** Distance between two selected carbon atoms in the imidazolium ring and in the alkyl chain, C2 and C9, in C₄mim⁺ cations in gauche (full line) or anti (dashed line) conformations.

Conclusions

The present study showed that structural information about the existence of different cation conformers obtained from MD simulations using a molecular force field is consistent with the same type of information extracted from experimental data (Raman spectroscopy) or theoretical calculations (ab initio methods). Therefore, we can conclude that the use of a molecular force field for ILs, in which the torsion parameters of the alkyl side chains attached to the imidazolium ring were specifically calculated,¹ has a paramount importance in accurately accounting for the conformational and structural features of the ionic liquids by molecular simulation.

The confrontation between simulation and liquid-phase spectroscopic evidence, apart from providing a partial validation of the force field used for the simulations, can also offer an overall view on the arrangement of the alkyl chain in 1-alkyl-3-methylimidazolium cations composing ionic liquids. The MD results showed that, as one proceeds from the dihedrals closer to the imidazolium ring to those approaching the end of the alkyl chain, the conformations become defined in a sharper manner: the dihedral centered around N1–C6 exhibits a wide distribution of possible conformations, the one centered at C6–C7 exhibits two possible conformers (anti or gauche) whereas those centered on C–C bonds beyond are predominately in an anti conformation. The simulations also showed that the planar conformation of the C7 carbon of the side chain relative to the imidazolium ring, which corresponds to a relative probability maximum in C₂mim⁺, is no longer present as a preferred conformers in alkylmethylimidazolium cations with longer side chains.

This picture is consistent with the statement in Berg et al.⁹ (and corroborated by other studies) that “the 1-alkyl-3-methylimidazolium cation will form, often multiple, hydrogen bonds from the cations usually with the H(C2), H(C4), H(C5), H(C6) and the terminal methyl group on the alkyl chains to even weak hydrogen bond acceptors, such as tetrafluoroborate and hexafluorophosphate”. In C₂mim⁺, the C7 (a terminal methyl group) adopts a planar conformation because in such case it will interact with an anion that is also interacting with H(C2). The C7 carbon loses its nature of terminal methyl group in longer alkylmethylimidazolium cations, and the preference for a planar conformation is also lost.

The coexistence of conformers (anti and gauche) around the C6–C7 bond in cations larger than [C₂mim]⁺ can also be interpreted as an attempt to bring the alkyl chain closer to the imidazolium ring, where stronger interactions with anions are

possible. This statement is confirmed by the two histograms in Figure 4 where the normalized distribution of the C2–C9 distances for the gauche and the anti conformations in [C₄mim]-[BF₄] are shown.

Acknowledgment. We thank Dr. Rolf W. Berg for sending us the original Raman spectra (ref 9). This work was supported by the French–Portuguese collaboration program PICS 3090 between CNRS and GRICES.

References and Notes

- (1) Canongia Lopes, J. N.; Deschamps, J.; Pádua, A. A. H. *J. Phys. Chem. B* **2004**, *108*, 2038; *J. Phys. Chem. B* **2004**, *108*, 11250.
- (2) Liu, Z. P.; Huang, S. P.; Wang, W. C. *J. Phys. Chem. B* **2004**, *108*, 12978.
- (3) Hanke, C. G.; Price, S. L.; Lynden-Bell R. M. *Mol. Phys.* **2001**, *99*, 801.
- (4) Morrow, T. I.; Maginn, E. *J. Phys. Chem. B* **2002**, *106*, 12807.
- (5) Urahata, S. M.; Ribeiro, M. C. C. *J. Chem. Phys.* **2004**, *120*, 1855.
- (6) Umebayashi, Y.; Fujimori, T.; Sukizaki, T.; Asada, M.; Fujii, K.; Kanzaki, R.; Ishiguro, S. *J. Phys. Chem. A* **2005**, *109*, 8976.
- (7) Ozawa, R.; Hayashi S.; Saha, S.; Kobayashi, A.; Hamagushi, H. *Chem. Lett.* **2003**, *32*, 948.
- (8) Katayanagi, H.; Hayashi, S.; Hamagushi, H.; Nishikawa, K. *Chem. Phys. Lett.* **2004**, *392*, 460.
- (9) Berg, R. W.; Deetlefs, M.; Seddon, K. R.; Shim, I.; Thomson, J. M. *J. Phys. Chem. B* **2005**, *109*, 19018.
- (10) Canongia Lopes, J. N.; Pádua, A. A. H. *J. Phys. Chem. B* **2004**, *108*, 16893.
- (11) Smith, W.; Forester, T. R. *The DL_POLY Package of Molecular Simulation Routines*, version 2.13; The Council for the Central Laboratory of Research Councils, Daresbury Laboratory: Warrington, U.K., 1999.
- (12) Jorgensen, W. L.; Maxwell, D. S.; Tirado-Rives, J. *J. Am. Chem. Soc.* **1996**, *118*, 11225. Kaminski, G.; Jorgensen, W. L. *J. Phys. Chem.* **1996**, *100*, 18010.
- (13) Margulis, C.; Stern, H. A.; Berne, B. J. *J. Phys. Chem. B* **2002**, *106*, 12017; Margulis, C. *Mol. Phys.* **2004**, *102*, 829.